Annals of Biomedical Engineering, Vol. 47, No. 6, June 2019 *(© 2019)* pp. 1400–1408
https://doi.org/10.1007/s10439-019-02245-w

The Effects of 4%Fe on the Performance of Pure Zinc as Biodegradable Implant Material

ALON KAFRI,[1] SHIRA OVADIA,[2] GALIT YOSAFOVICH-DOITCH,[2] and ELI AGHION[1]

[1]Department of Materials Engineering, Ben-Gurion University of the Negev, 8410501 Beer-Sheva, Israel; and [2]Faculty of Health Science, Ben-Gurion University of the Negev, 8410501 Beer-Sheva, Israel

(Received 7 January 2019; accepted 6 March 2019; published online 8 March 2019)

Associate Editor Jennifer West oversaw the review of this article.

Abstract—The efforts to develop structural materials for biodegradable metal implants have lately shifted their focus from Magnesium and Iron base alloys towards Zinc. This was mainly due to the accelerated corrosion rate of Mg that is accompanied by hydrogen gas evolution, formation of voluminous iron oxide products with reduced degradation rate in the case of Iron implants and the crucial role of Zn in many physiological processes. However the mechanical properties and degradation capabilities of pure zinc in physiological environment are limited and do not comply with the requirements of biodegradable implants. The present study aims at evaluating the effect of 4%Fe on the *in-vitro* and *in-vivo* behavior of pure Zinc. This was carried out in order to address the inherent disadvantages of pure zinc in terms of mechanical properties and biodegradability. The results obtained clearly indicate that the biocompatibility and mechanical properties of the new material system was in accord with the prospective requirements of biodegradable implants. However the corrosion degradation of the new alloy in *in-vivo* conditions was quite similar to that of pure zinc in spite of the significant micro-galvanic effect created by Delta phase $Zn_{11}Fe$.

Keywords—Zinc, Biodegradable, Biocompatible, *In-vivo*, *In-vitro*, Corrosion degradation.

INTRODUCTION

Traditionally the research developments of biodegradable metal implants were mainly attributed to iron and magnesium base systems due to their inherent biocompatibility and suitable mechanical properties. In the case of iron base implants,[8,10,13,24,30] although iron corrodes at a reasonable rate it accumulates a voluminous corrosion product that repels neighboring cells and biological matrix and does not appear to be excreted or metabolized at an appreciable rate. The interest in Mg based implants[3,4,9,12,15,16,21,27,29,31,42] relates to their excellent biocompatibility, adequate mechanical properties, and their beneficial contribution to bone growth.[11,35,39,40] However, the degradation of Mg base systems in physiological environment encounter formation of hydrogen gas babbles that can lead to tissues separation and in rare cases gas embolism.[2,34]

In light of the inherent disadvantages of Mg and Fe, Zinc emerges as a promising implant element that naturally participate in numerous physiological process such as signal transduction, gene expression and nucleic acid metabolism.[5,17] However the main drawbacks of pure Zn as a biodegradable implant are poor mechanical properties,[6,7] risk of anemia and poor growth when high levels of Zn are found in the body,[26,33] and relatively reduced corrosion rate.[43] Hence, the improvement of the mechanical properties of Zn base alloys as well as controlling their corrosion rate while maintaining its biocompatibility was the main focus of several research activities.[1,18,22,23,25,32,36–38,41] The present study aims at evaluating the prospects of Zn-4%Fe alloy as a new structural material for biodegradable implants. This was based on the assumption that alloying Zn with Fe can enhance the corrosion rate of pure Zn by micro-galvanic effect as well as improving the mechanical properties by solid solution and phase precipitation while maintaining the implant's biocompatibility.

MATERIALS AND METHODS

The Zn base alloy used by this study was of Zn-4%Fe, produced by gravity casting process followed by machining from the central part of the cast ingot.

Address correspondence to Alon Kafri, Department of Materials Engineering, Ben-Gurion University of the Negev, 8410501 Beer-Sheva, Israel. Electronic mails: kafria@bgu.ac.il, Kafri09@gmail.com

The full chemical composition of that alloy as obtained by an Inductively Coupled Plasma Optical Emission Spectrometer (ICP-SPECTRO, ARCOS FHS-12) reveal 4.105 of Fe, 0.0014 of Pb, 0.0045 of Al, 0.0017 of Cu and less than 0.0002 of Cd, all in wt%.

The microstructure examination was obtained by scanning electron microscopy (SEM) using JEOL JSM-5600 (JEOL, Tokyo, Japan) with an energy dispersive spectrometer (EDS) detector (Thermo fisher scientific, Ma, USA). Phase identification was carried out using an X-ray diffractometer RIGAKU-2100H (RIGAKU, Tokyo, Japan) with Cu-Kα radiation. Diffraction parameters were 40 kV/30 mA and the scanning rate was 2°/min.

Vickers hardness measurements were obtained using a Zwick/Roell Indentec-Quantarad Technologies and the tensile tests after subsequent extrusion were done using a CORMET slow strain rate machine (C76, Finland) at a rate of 0.5 mm/min. tensile test specimen were with a gauge length of 16 mm and a diameter of 4 mm in accordance with ASTM E8 standard.

The *in-vitro* environmental behavior of the Zn-4%Fe alloy was examined by an immersion test performed in a phosphate-buffered saline (PBS) solution at 37 °C with pH level of ~ 7.4 for up to 30 days according to ASTM G31-12a standard. The corrosion products post immersions were removed using a 10% NH_4Cl solution according to ASTM G1-03 standard procedure. Electrochemical behavior in terms of electrochemical impedance spectroscopy (EIS) was conducted using a Bio-Logic SP-200 potentiostat equipped with EC-Lab software. The corrosion chamber for the electrochemical testing was composed of a three-electrode cell system having a calomel reference electrode (SCE), a platinum counter electrode, and the tested sample as the working electrode. The exposed area of the working electrode was 1 cm^2 while the EIS testing was carried out between 10 kHz and 100 mHz at 10 mV amplitude over the open circuit potential. Prior to electrochemical testing, the samples were polished up to 2500 grit, cleaned in an ultrasonic bath for 5 min, washed with alcohol, and dried in hot air.

The samples used for the *in-vivo* experiments were the Zn-4%Fe alloy and Ti-6Al-4 V as a reference metal. The *in-vivo* behavior was evaluated over a period of 6 months using metal implantations in the form of 2 cylindrical discs (7 mm diameter and 2 mm height) implanted in males Wistar rats. The implantation procedure included 6 rats with Zn-4%Fe implants ($n = 6$) and 6 rats with Ti-6Al-4 V implants ($n = 6$). The rats were anesthetized using Isoflurane (Terrel TM Piramal Critical Care, Inc, Bethlehem PA, USA) followed by aseptically implantation subcutaneously in the midline of the back of the rats, one between scapula's and another in mid-lumbar area. Post implantation procedure included daily monitoring of the incision area, locomotion in cage and general wellbeing behavior of the rats during the first week. This was followed by weekly evaluation of the rats' body weight and their wellbeing behavior. Routinely, every 4 weeks blood was collected from the retro-orbital sinus. Whole blood (1 mL) was collected in EDTA for a complete blood count (CBC) for red blood cells (RBC), hemoglobin (HGB) and white blood cells (WBC). Serum (1 mL) was collected for determination of Zn levels. At week 14 post implantation half of the rats in each group were euthanized with intraperitoneal 150 mg/kg Pentobarbital (CTS Chemical Industries Ltd, Hod Hasharon, Israel) for alloy and tissue harvest. Tissue from each alloy location was placed in 10% formaldehyde for histology. Histological analysis of tissues surrounding the implants was examined in order to evaluate possible inflammation, necrosis and tissue fibrosis. Samples were trimmed, embedded in paraffin and stained with hematoxylin & eosin (H&E) and assessed blindly by a veterinary pathologist (Patho-Logica, Ness Ziona, Israel).

In order to evaluate the *in-vivo* corrosion rate, the corrosion products were removed and weighted using the same 10% NH_4Cl solution used in the *in-vitro* tests.

All the animal experiments were approved by the Ben-Gurion University of the Negev (BGU) Committee for the Ethical Care and Use of Laboratory Animals (BGU-IACUC). The experiments were performed according to the Israel Animal Welfare law (1994) and the NRC Guide for the Care and Use of Laboratory Animals (2011). BGU's animal care and use program is approved by the Association for the Assessment and Accreditation of Laboratory Animal Care International (AAALAC). The *in vivo* experiments were carried out at BGU rodent facility. Twelve 250 g male Wistar rats (Envigo, Jerusalem, Israel) were selected for the *in vivo* assessment.

RESULTS

Typical microstructure and spot chemical composition analysis of Zn-4%Fe alloy obtained by SEM and EDS detection is shown in Fig. 1a. This has revealed a Zn base matrix with a second Fe-rich phase that was scattered evenly across the entire bulk material. The Fe content in the Fe-rich phase was between 9 and 11 wt% indicating that the second phase is Zn-delta phase.[14] The X-ray diffraction analysis revealed the presence of two major phases: pure Zn and Fe-rich phase as shown in Fig. 1b. The Fe-rich phase was identified as $Zn_{11}Fe$ (according to ICDD 045-1184) which comes in line with the EDS detection shown in Fig. 1a. Both examinations clearly indicate that the Fe-rich phase is Zn-Delta phase.

In order to evaluate the mechanical properties of the Zn-base alloy following gravity casting and hot

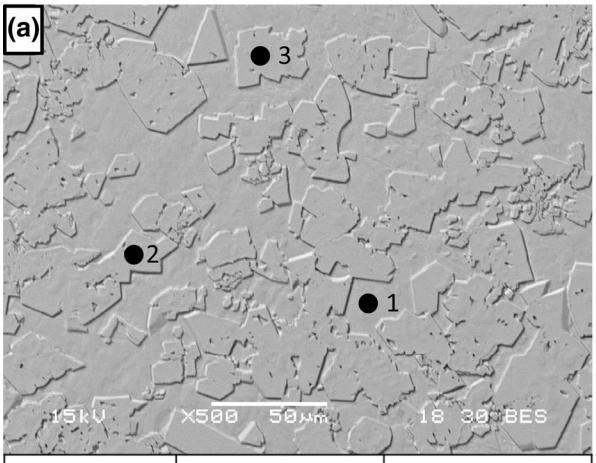

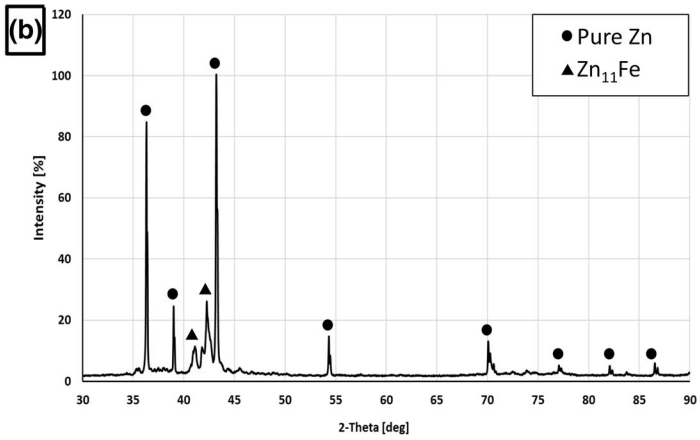

	Zn	Fe
Point 1	100	0
Point 2	90.2±1.17	9.8±0.28
Point 3	89.13±1.04	10.87±0.25

FIGURE 1. Typical microstructure and X-ray diffraction analysis of Zn-4%Fe alloy (a) Microstructure at a close-up view with locations of spot chemical composition analysis; (b) Diffraction analysis.

extrusion, hardness and tensile test were conducted. The hardness of the Zn-4%Fe alloy was 87 ± 4 HV (hardness Vickers) compared to pure Zn hardness of 40 ± 3. Tensile test results reveal a significant improvement in mechanical properties compared to pure Zn: uniaxial tensile strength (UTS) of 126.4 ± 4.8 MPa, yield strength (YS) of 96 ± 4.1 MPa and elongation (%E) of 12.4 ± 1.6 in comparison with the pure Zn properties of UTS of 52.8 ± 6.9, YS of 44.8 ± 2.7 and %E of 4.8 ± 0.3. This have revealed adequate mechanical properties as biodegradable metal implant that comes in line with the basic mechanical requirements of implants for orthopedic and cardiovascular applications. The relatively high elongation value is attributed to the beneficial effects of the extrusion process.

Immersion test for up to 30 days revealed a general corrosion attack with decreasing corrosion rate of the Zn-4%Fe alloy compared to pure Zn as shown in Fig. 2a. The relatively reduced corrosion rate of the Zn-4%Fe alloy in time can be attributed to the extensive production of corrosion products that may provide some type of passivation effect to the alloy. Close-up views at a cross section of the corroded alloy after the removal of corrosion products was carried out in order to understand the corrosion mechanism. This has revealed a uniform corrosion attack as can be clearly seen in Fig. 2a. Close-up examinations shown in Figs. 2c and 2d indicated that the Fe-rich phase (Delta phase) was relatively un-attacked compared to the corroded Zn matrix. This can explain the increased corrosion rate of Zn-4%Fe alloy compared to Pure Zn that is generated due to the micro-galvanic effect produced by the Delta phase.[18,19]

Electrochemical behavior by EIS carried out in PBS solution is shown in Figs. 3a and 3b in terms of Nyquist and Bode plot respectively. Different exposure times were used in order to explore the effect of exposure time on the decrease in corrosion rate of the alloy. The EIS analysis in terms of Nyquist examination indicated an improved corrosion resistance as implied by the larger radius curvature of the 12 h exposure line. Bode plot analysis showed increased corrosion resistance with time as seen by the interception of the bode line with Y-axis. This increase in corrosion resistance over time (7744 Ohm at 1 h, 10447 Ohm at 6 h and 15885 Ohm at 12 h) may explain the decrease in corrosion rate calculated from the immersion test as a function of time. Electrical equivalent circuit (EEC) was fitted based on the Nyquist plots as shown in Fig. 3c. While the same circuit model was fitted to all exposure times, the variations in the component values were significant. This relates to R_S—solution resistance between the reference electrode and the working electrode, R_{dl}—a constant phase element, Q_{dl}—relates to the double layer, R_{dl}—charge transfer resistance related to the electrochemical reaction and the Q_{dl} component related to the capacitance of the double layer.[20,23] Constant phase elements such as Q_{dl} are governed by the exponent a,

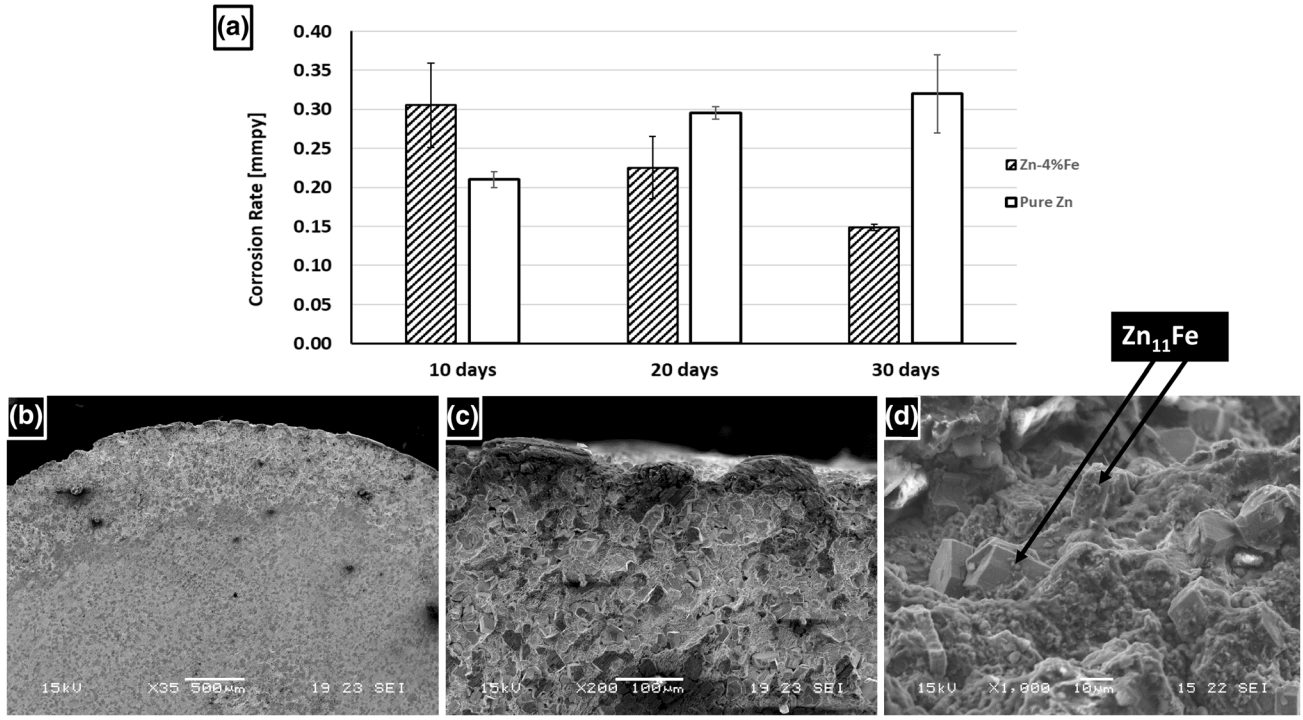

FIGURE 2. Corrosion rate measurements and cross section view of pure Zn and Zn-4%Fe alloy after immersion test in PBS solution at 37 °C; (a) Corrosion rate vs. exposure time (b) general cross section view (c, d) close-up view of corrosion degradation.

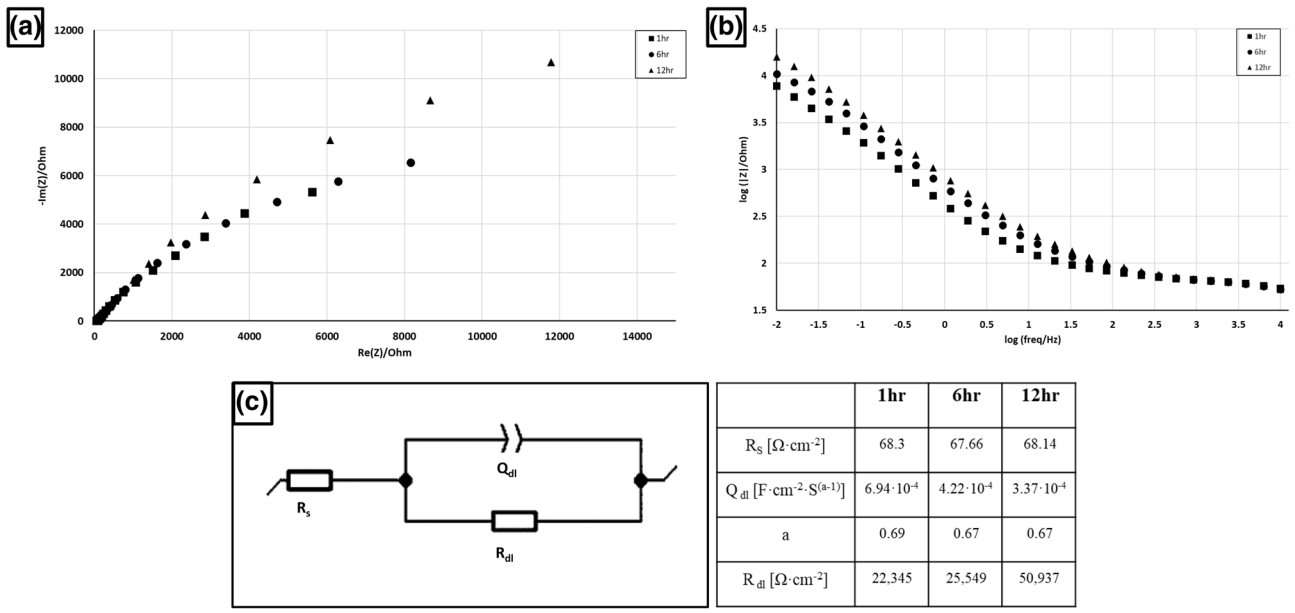

	1hr	6hr	12hr
R_S [Ω·cm^{-2}]	68.3	67.66	68.14
Q_{dl} [F·cm^{-2}·S$^{(a-1)}$]	$6.94 \cdot 10^{-4}$	$4.22 \cdot 10^{-4}$	$3.37 \cdot 10^{-4}$
a	0.69	0.67	0.67
R_{dl} [Ω·cm^{-2}]	22,345	25,549	50,937

FIGURE 3. Nyquist and Bode plots obtained after immersion of Zn-4%Fe alloy in PBS solution after 1, 6 and 12 h; (a) Nyquist plot (b) Bode plot (c) Electrical equivalent circuit.

where $a = 1$ indicates an ideal capacitor C. As predicted, the solution resistance of all tested samples is the same and the double layer capacitance is in the same order magnitude. On the other hand, the values of the charge transfer resistor, R_{dl} increases rapidly over time, more than twice in 12 h of exposure. Overall, the result of the EIS analysis corresponds with the corrosion rate calculated by the immersion tests.

Relating to *in-vivo* examinations the influence of the Zn-4%Fe implant on the wellbeing of the rats is rep-

resented by the normal weight gain in comparison to the weight gain of the control group, as seen in Fig. 4a. Weekly monitoring of the animal behavior, locomotion in cage and the appearance of the surgical incision showed no sign of negative or harmful effects generated by the Zn-4%Fe implants. Serum Zinc levels before and post implantation are shown in Fig. 4b. The slightly increased Zn serum levels, in the rats implanted with the Zn-4%Fe alloy compared to the rats implanted with titanium alloy, are within the normal range of 168–190 [μg/dL].[44]

Prior to the sacrificing of the rats, radiographic images were taken from rats with Zn-base and Ti-6Al-4 V implants, in order to disclose any traces of hydrogen gas forming during the degradation of the implants. Typical images have clearly indicated that no gas evolution occurred during the 24 weeks of implantation as shown in Fig. 5.

Analysis of blood sampled in terms of RBC, HGB and WBC levels before implantation and up to 24 weeks post implantation are shown in Fig. 6. In addition, all the tested biochemical parameters were all within normal range[28]: RBC 7.62–9.99 [10*6/μL], HGB 13.6–17.4 [g/dL] and WBC 1.98–11.06 [10*3/μL]. These findings suggest that no harmful effect was developed as a result of Zn-4%Fe alloy implantations.

In order to evaluate the corrosion rate of the implants in *in-vivo* conditions the corrosion products formed on the external surface of the implants were removed and measured against the original weight of the implants. The calculated corrosion rate of Zn-4%Fe alloy exhibits a decrease over time as were the corrosion rate of Zn-4%Fe after 14 weeks was 0.063 ± 0.009 mm/y compared to 0.033 ± 0.009 mm/year after 24 weeks. Although this result comes in line with the *in-vitro* results shown earlier it should be pointed out that relatively reduced amount of Fe (about 2%) in Zn–Fe system has a reverse trend as discovered by a previous paper of the authors.[18]

Histological analysis of subcutaneous tissues located close to the metals implants is shown in Fig. 7. No signs of inflammation or necrosis were evident in

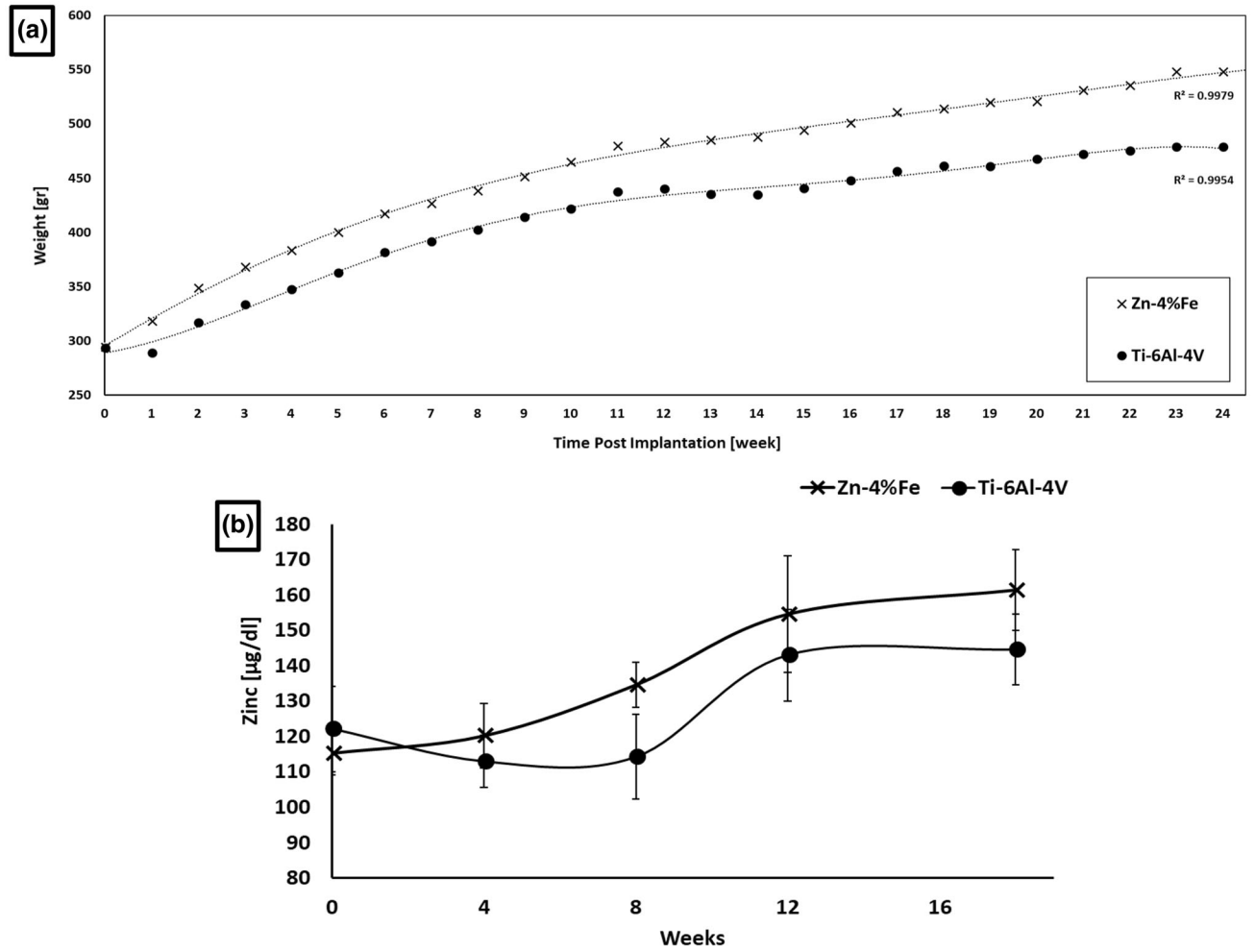

FIGURE 4. Rat body weight and Serum Zinc level vs. time (post-implantation); (a) Body weight (b) Serum Zinc level.

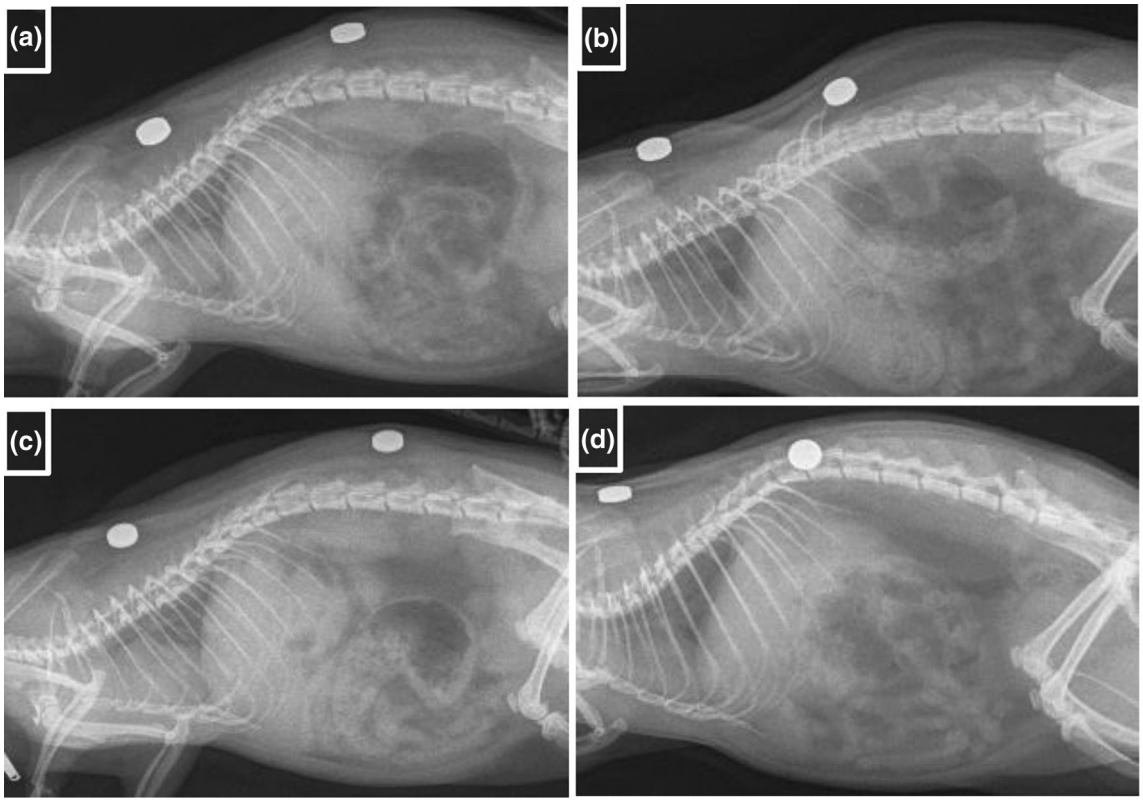

FIGURE 5. Radiographic assessment of rats with metal implants; (a, b) Zn-4%Fe implants after 14 and 24 weeks post-implantation respectively. (c, d) Ti-6Al-4 V implants after 14 and 24 weeks post-implantation respectively.

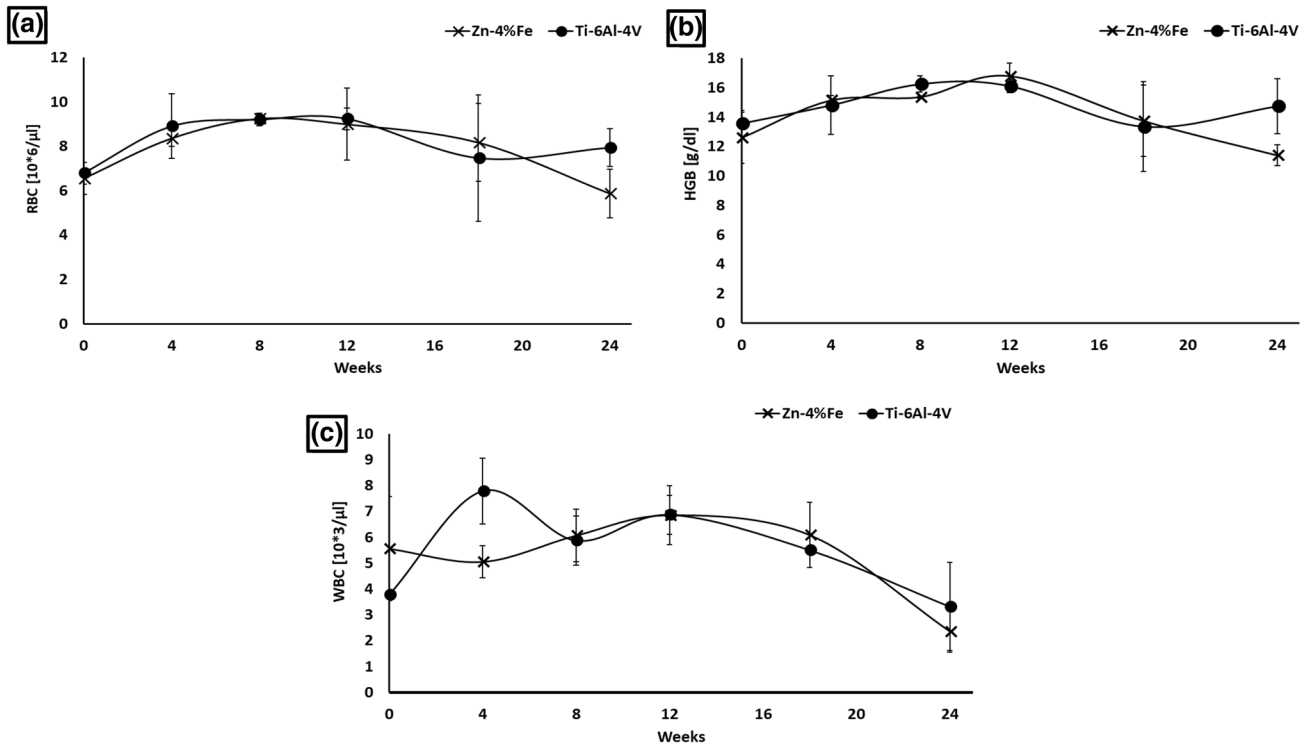

FIGURE 6. Blood biochemistry test vs. time (post-implantation); (a) Red blood cells (RBC) level (b) Hemoglobin (HGB) level (c) White blood cells (WBC) level.

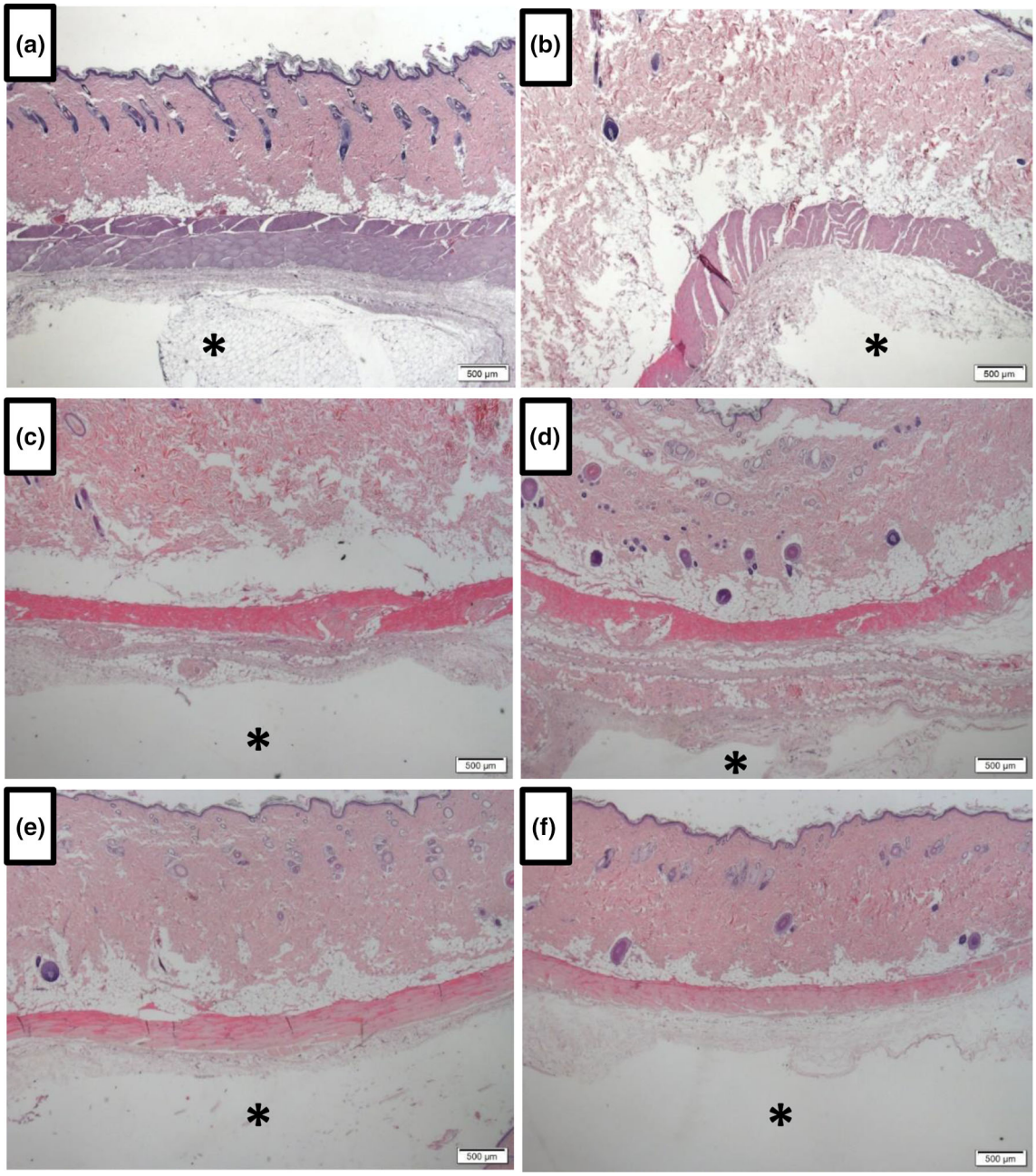

FIGURE 7. Histological analysis at subcutaneous tissues (harvested from cranial and caudal orientation) located in the vicinity of the implanted metals (marked by asterisks), 14 and 24 weeks post-implantation; (a, b) Zn-4%Fe implants 14 weeks post-implantation, (c,d) Zn-4%Fe implants 24 weeks post-implantation. (e, f) Ti-6Al-4 V implants 24 weeks post-implantation.

any of the tested tissues close to the Zn-4%Fe and Ti6Al4 V metal implants. This clearly indicates that no detrimental effect is being generated by the presence of Zn-4%Fe implant and its corrosion products during normal *in-vivo* degradation conditions. In addition, comparing tissues originated form the same rat, no marked differences were observed, suggesting that the location of the implant within the rat (cranial or caudal) was insignificant in this case.

DISCUSSION

The results obtained by the *in-vivo* assessment post implantation in terms of rat's weight gain, level of serum Zn, red blood cells, hemoglobin, white blood cells and histological analysis clearly indicate that Zn-4%Fe alloy can be considered as a biocompatible implant material. This was also supported by the radiographic assessment that showed no evidence of

hydrogen gas evolution as in the case of biodegradable Mg based implants.[16] The corrosion rate of this alloy in *in-vivo* conditions after 14 and 24 weeks post implantation was quite similar to that of pure Zn.[18] This result indicate that the addition of 4%Fe did not accelerate the corrosion rate of pure Zn as required in order that the alloy can be considered as an acceptable biodegradable material. The nature of this result was also highlighted by the *in-vitro* assessment that showed that although the relatively corrosion rate of Zn-4%Fe was increased after 10 days post implantation, this tendency was reversed after 20 and 30 days where the corrosion rate of pure zinc was even higher. This outcome was not in line with our previous results[18] when the amount of Fe was reduced to just about 2% and the corrosion rate was considerably increased compared to pure Zinc.

Hence it is believed that the excess amount of iron in Zn-Fe alloy (4%Fe vs. 2%Fe) resulted in increased corrosion rate after initial exposure to physiological environment that consequently created some form of passivation behavior. This assumption was also supported by the EIS assessment in terms of Nyquist examination and Bode plot analysis that showed improved corrosion resistance as exposure time increased (Fig. 3). Probably the accelerated formation of corrosion products was generated due to relatively excessive amount of Delta phase ($Zn_{11}Fe$) that have a significant micro-galvanic effect in relation to the zinc matrix. This was clearly evident from the examination of the corrosion attack surface (Fig. 2d) that showed that Delta phase was nearly un-attacked compared to the corroded Zn matrix.

The mechanical behavior the Zn-4%Fe alloy showed acceptable properties as implant material for orthopedic applications. This was demonstrated in terms of yield strength and elongation, 126 MPa and 12% respectively vs. typical bone properties: 104 MPa yield strength and above 5% elongation,[22] As for cardiovascular applications and stents in particular the obtained mechanical properties of Zn-4%Fe also comes in line with the basic mechanical requirements as indicated by Bowen *et al.*[10]

Altogether although the properties of Zn-4%Fe alloy as a structural material for biodegradable implant applications in terms of biocompatibility and mechanical properties are acceptable its corrosion degradation in *in-vivo* conditions do not introduce any advantage compared to pure zinc. Consequently, as the corrosion rate of pure Zinc is currently too low for practical biodegradable implants the applicability of Zn-4%Fe alloy is limited and do not address the degradability requirements as obtained by Zn-Fe systems with reduced amount of iron.

REFERENCES

[1]Aghion, E. Biodegradable metals. *Metals (Basel)* 8(10):804, 2018.

[2]Aghion, E., and G. Levy. The effect of Ca on the in vitro corrosion performance of biodegradable Mg-Nd-Y-Zr alloy. *J. Mater. Sci.* 45(11):3096–3101, 2010.

[3]Aghion, E., G. Levy, and S. Ovadia. *In vivo* behavior of biodegradable Mg-Nd-Y-Zr-Ca alloy. *J. Mater. Sci. Mater. Med.* 23(3):805–812, 2012.

[4]Aghion, E., T. Yered, Y. Perez, and Y. Gueta. The prospects of carrying and releasing drugs via biodegradable magnesium foam. *Adv. Eng. Mater.* 12(8):B374–B379, 2010.

[5]Al-Maroof, R. A., and S. S. Al-Sharbatti. Serum zinc levels in diabetic patients and effect of zinc supplementation on glycemic control of type 2 diabetics. *Saudi Med. J.* 27(3):344–350, 2006.

[6]Bakhsheshi-Rad, H. R., *et al.* Fabrication of biodegradable Zn-Al-Mg alloy: mechanical properties, corrosion behavior, cytotoxicity and antibacterial activities. *Mater. Sci. Eng. C* 73:215–219, 2017.

[7]Bakhsheshi-Rad, H. R., *et al.* Thermal characteristics, mechanical properties, in vitro degradation and cytotoxicity of novel biodegradable Zn–Al–Mg and Zn–Al–Mg–xBi alloys. *Acta Metall. Sin.* 30(3):201–211, 2017.

[8]Boland, E. L., R. Shine, N. Kelly, C. A. Sweeney, and P. E. McHugh. A review of material degradation modelling for the analysis and design of bioabsorbable stents. *Ann. Biomed. Eng.* 44(2):341–356, 2016.

[9]Bowen, P. K., J. Drelich, R. E. Buxbaum, R. M. Rajachar, and J. Goldman. New approaches in evaluating metallic candidates for bioabsorbable stents. *Emerg. Mater. Res.* 1(5):237–255, 2012.

[10]Bowen, P. K., *et al.* Biodegradable metals for cardiovascular stents: from clinical concerns to recent Zn-alloys. *Adv. Healthc. Mater.* 5(10):1121–1140, 2016.

[11]Brar, H. S., M. O. Platt, M. Sarntinoranont, P. I. Martin, and M. V. Manuel. Magnesium as a biodegradable and bioabsorbable material for medical implants. *JOM* 61(9):31–34, 2009.

[12]Elkaiam, L., O. Hakimi, J. Goldman, and E. Aghion. The effect of Nd on mechanical properties and corrosion performance of biodegradable Mg-5%Zn alloy. *Metals (Basel)* 8(6):438, 2018.

[13]Feng, Q., *et al.* Characterization and in vivo evaluation of a bio-corrodible nitrided iron stent. *J. Mater. Sci. Mater. Med.* 24(3):713–724, 2013.

[14]Fransen, M., and C. Nazikkol. Zinc / iron phase transformation studies on galvannealed steel coatings by X-ray diffraction. *Advances* 46:291–296, 2003.

[15]Hakimi, O., and E. Aghion. Corrosion performance of biodegradable Mg-6%Nd-2%Y-0.5%Zr produced by melt spinning technology. *Adv. Eng. Mater.* 16(4):364–370, 2014.

[16]Hakimi, O., E. Aghion, and J. Goldman. Improved stress corrosion cracking resistance of a novel biodegradable EW62 magnesium alloy by rapid solidification, in simulated electrolytes. *Mater. Sci. Eng. C* 51:226–232, 2015.

[17]Hambidge, K. M., and N. F. Krebs. Zinc deficiency: a special challenge. *J. Nutr.* 137(4):1101–1105, 2007.

[18]Kafri, A., S. Ovadia, G. Yosafovich-Doitch, and E. Aghion. In vivo performances of pure Zn and Zn–Fe alloy as biodegradable implants. *J. Mater. Sci. Mater. Med.* 29(7):94, 2018.

[19]Lee, H. H., and D. Hiam. Corrosion resistance of galvannealed steel. *Corrosion* 45(10):852–856, 1989.
[20]Leon, A., and E. Aghion. Effect of surface roughness on corrosion fatigue performance of AlSi10 Mg alloy produced by Selective Laser Melting (SLM). *Mater. Charact.* 131:188–194, 2017.
[21]Levy, G. K. and E. Aghion. Improving the corrosion resistance of biodegradable magnesium alloys by diffusion coating process. In: Magnesium Technology, 2015.
[22]Levy, G. K., J. Goldman, and E. Aghion. The prospects of zinc as a structural material for biodegradable implants—a review paper. *Metals (Basel)*. 7(10):402, 2017.
[23]Levy, G. K., *et al*. Evaluation of biodegradable Zn-1%Mg and Zn-1%Mg-0.5%Ca alloys for biomedical applications. *J. Mater. Sci. Mater. Med* 28:11–174, 2017.
[24]Liu, B., and Y. F. Zheng. Effects of alloying elements (Mn Co, Al, W, Sn, B, C and S) on biodegradability and in vitro biocompatibility of pure iron. *Acta Biomater.* 7(3):1407–1420, 2011.
[25]Mostaed, E., *et al*. Novel Zn-based alloys for biodegradable stent applications: design, development and in vitro degradation. *J. Mech. Behav. Biomed. Mater.* 60:581–602, 2016.
[26]Piao, F., K. Yokoyama, N. Ma, and T. Yamauchi. Subacute toxic effects of zinc on various tissues and organs of rats. *Toxicol. Lett.* 145(1):28–35, 2003.
[27]Pierson, D., *et al*. A simplified in vivo approach for evaluating the bioabsorbable behavior of candidate stent materials. *J. Biomed. Mater. Res. Part B.* 100(1):58–67, 2012.
[28]Quesenberry, K. E., and J. W. Carpenter. Small rodents. Ferrets, Rabbits and Rodents: Clinical Medicine and Surgery, 2003, p. 348.
[29]Razavi, M., M. Fathi, O. Savabi, D. Vashaee, and L. Tayebi. Improvement of biodegradability, bioactivity, mechanical integrity and cytocompatibility behavior of biodegradable mg based orthopedic implants using nanostructured bredigite (Ca7MgSi4O16) bioceramic coated via ASD/EPD technique. *Ann. Biomed. Eng.* 42(12):2537–2550, 2014.
[30]Schinhammer, M., A. C. Hänzi, J. F. Löffler, and P. J. Uggowitzer. Design strategy for biodegradable Fe-based alloys for medical applications. *Acta Biomater.* 6(5):1705–1713, 2010.
[31]Schümann, K., T. Ettle, B. Szegner, B. Elsenhans, and N. W. Solomons. On risks and benefits of iron supplementation recommendations for iron intake revisited. *J. Trace Elem. Med. Biol.* 21(3):147–168, 2007.
[32]Sikora-Jasinska, M., E. Mostaed, A. Mostaed, R. Beanland, D. Mantovani, and M. Vedani. Fabrication, mechanical properties and in vitro degradation behavior of newly developed Zn Ag alloys for degradable implant applications. *Mater. Sci. Eng. C* 77:1170–1181, 2017.
[33]Smith, S. E., and E. J. Lakson. Zinc toxicity in rats; antagonistic effects of copper and liver. *J. Biol. Chem.* 163:29–38, 1946.
[34]Song, G. Control of biodegradation of biocompatable magnesium alloys. *Corros. Sci.* 49(4):1696–1701, 2007.
[35]Song, G., and S. Song. A possible biodegradable magnesium implant material. *Adv. Eng. Mater.* 9(4):298–302, 2007.
[36]Tang, Z., *et al*. Design and characterizations of novel biodegradable Zn-Cu-Mg alloys for potential biodegradable implants. *Mater. Des.* 117:84–94, 2017.
[37]Vojtěch, D., J. Kubásek, J. Šerák, and P. Novák. Mechanical and corrosion properties of newly developed biodegradable Zn-based alloys for bone fixation. *Acta Biomater.* 7(9):3515–3522, 2011.
[38]Wang, C., H. T. Yang, X. Li, and Y. F. Zheng. In vitro evaluation of the feasibility of commercial Zn alloys as biodegradable metals. *J. Mater. Sci. Technol.* 32(9):909–918, 2016.
[39]Witte, F., H. Ulrich, C. Palm, and E. Willbold. Biodegradable magnesium scaffolds. Part II. Peri-implant bone remodeling. *J. Biomed. Mater. Res. Part A* 81(3):757–765, 2007.
[40]Witte, F., H. Ulrich, M. Rudert, and E. Willbold. Biodegradable magnesium scaffolds. Part I. Appropriate inflammatory response. *J. Biomed. Mater. Res. Part A* 81(3):748–756, 2007.
[41]Xiao, C., *et al*. Indirectly extruded biodegradable Zn-0.05 wt%Mg alloy with improved strength and ductility: in vitro and in vivo studies. *J. Mater. Sci. Technol.* 34(9):1618–1627, 2018.
[42]Yang, J., J. L. Guo, A. G. Mikos, C. He, and G. Cheng. Material processing and design of biodegradable metal matrix composites for biomedical applications. *Ann. Biomed. Eng.* 46(9):1229–1240, 2018.
[43]Yue, R., *et al*. Microstructure, mechanical properties and in vitro degradation behavior of novel Zn-Cu-Fe alloys. *Mater. Charact.* 134:114–122, 2017.
[44]Yur, F., A. Bildik, F. Belge, and D. Kilicalp. Serum plasma and erythrocyte zinc levels in various animal species. *VAN Vet. J.* 13:82–83, 2002.